Korean J. Chem. Eng., 36(3), 456-467 (2019)
DOI: 10.1007/s11814-018-0196-4

pISSN: 0256-1115
eISSN: 1975-7220

Reactive insights into the hydrogen production from ammonia borane facilitated by phosphonium based ionic liquid

Debashis Kundu*, Sankar Chakma, Gopal Pugazhenthi*, and Tamal Banerjee*,†**

*Department of Chemical Engineering, Indian Institute of Technology Guwahati, Guwahati -781039, Assam, India
**Department of Chemical Engineering, Indian Institute of Science Education and Research Bhopal, Bhopal - 462 066, Madhya Pradesh, India
(*Received 27 August 2018 • accepted 25 November 2018*)

Abstract−The current work presents a mechanistic insight of hydrogen production from ammonia borane (AB) facilitated by the phosphonium based ionic liquid (IL), trihexyl(tetradecyl)phosphonium bis (2,4,4-trimethylpentyl) phosphinate ([TDTHP][Phosph]). Prior to experiments, the IL was screened from a pool of 11 phosphonium ILs with the infinite dilution activity coefficients (IDAC) values as predicted by conductor like screening model segment activity coefficient (COSMO-SAC) theory. Thereafter, a dehydrogenation experiment of AB/[TDTHP][Phosph] was carried out at 105 °C and 4×10^{-2} mbar of gauge pressure, which yielded 2.07 equivalent hydrogen production. At higher temperature, the ^{11}B NMR characterization shows the suppression of induction period at 105 °C and appearance of borohydride anion after 1 min of dehydrogenation. Further, time-resolved characterization of AB/[TDTHP][Phosph] at 105 °C confirmed the appearance of polymeric aminoborane after 10 min with a subsequent formation of polyborazylene. HR-MS characterization coupled with ^{1}H resonance spectrum confirmed structural integrity of IL. The dual characterization of NMR and HR-MS led us to propose a dehydrogenation mechanism of AB/[TDTHP][Phosph] system.

Keywords: Ammonia Borane, Phosphonium Ionic Liquid, Boron NMR, COSMO-SAC

INTRODUCTION

Amine boranes are composed of boron, nitrogen and hydrogen with at least one B-N covalent bonding. This class of compounds is considered as potential storage of hydrogen which can be released by heating, solvation or catalysis. The simplest amine borane is ammonia borane (AB), having gravimetric hydrogen storage capacity of 19.6 wt%. Solid AB, being tetragonal, has interatomic distance between two hydrogens as 2.02 Å, implying the existence of dihydrogen bonding network [1,2]. It starts to release hydrogen (H_2) at 85 °C with prolong heating. Thermal dehydrogenation of AB is generally considered uncontrolled in nature resulting in various by-product formation and distribution. Additionally, it releases volatiles like borazine and ammonia, which are detrimental for fuel cell applications [3]. Although ammonia is a potential energy carrier, a renewable path for ammonia production is desired [4]. Partial dehydrogenation releases 2-2.5 equivalent hydrogen along with a series of volatile oligomers such as cyclotriborazane $(H_2NBH_2)_3$, aminodiborane ($NH_2B_2H_5$) and nonvolatile oligomers like polyaminoborane $[(NH_2BH_2)_n$, PAB], polyiminoborane $[(NHBH)_n$, PIB] and Polyborazylene $[(B_3N_3H_4)_n$, PB]. Complete dehydrogenation of AB leads to ceramic boron nitride, having a heat of formation of −107 Kcal mol^{-1} [5]. Therefore, to suppress the formation of volatiles and achieve milder dehydrogenation condition, several scaffolds such as transition metal catalysis [6], mesoporous silica [7], catalytic hydrolysis [8] and ionic liquids [9] are used. Among them, ionic liquids (ILs) as solvents have proven excellent stabilization of the AB intermediates. This has hence necessitated our attention towards these novel solvents as catalyst cum media for these reactions.

ILs are composed of organic cations and organic or inorganic anions. Tunable physio-chemical properties, nonvolatility, negligible vapor pressure, wide liquidus temperature, highly polar nature and its ability to form nonbonded interactions with other constituents make them preferred solvents over volatile organic solvent. Thus, it finds application in organic and inorganic synthesis [10], catalysis [11], biological systems [12] and separation media [13]. The pioneering work of Bluhm et al. reported the enhanced dehydrogenation of AB in 1-butyl-3-methyl imidazolim chloride {[BMIM][Cl]} IL without any induction period [14]. Later, Himmelberger et al. explored the dehydrogenation mechanism of AB/[BMIM][Cl] system with ^{11}B nuclear magnetic resonance (NMR) characterization [9]. The physical and structural properties such as density, viscosity, melting/freezing/glass transition temperature and solubility of AB/imidazolium IL systems are reported by Nakagawa et al. [15]. Ahluwalia et al. predicted the kinetics of AB/[BMIM][Cl] system by modified Avrami-Erofeyev model [16]. Mahato et al. further elaborated that kinetics of solid state AB follows growth propagation model, whereas Avrami-Erofeyev model is more appropriate for AB/IL systems [17]. Valero-Pedraza et al. reported dehydrogenation of AB in imidazolium, phophonium, choline and pyridinium classes of ILs [18]. Hydrophobic anions involving bis(trifluoromethylsulfonyl)imide anion based ILs are found to slow the dehydrogenation process. On the contrary, choline acetate is reported to release more than two equivalent of hydrogen after 20 hours of

†To whom correspondence should be addressed.
E-mail: tamalb@iitg.ac.in
Copyright by The Korean Institute of Chemical Engineers.

reaction. Recently, Gatto et al. employed pyrrolidinium and ammonium based hydrophobic ILs for the dehydrogenation of AB [19]. They obtained an enhanced hydrogen release below 90 °C in presence of air. Sahiner and Alpaslan reported dehydrogenation of AB in ionic liquid hydrogels containing cobalt, nickel and copper metal ions [20]. Wright et al. reported the transition metal catalyst supported dehydrogenation of AB/IL system [21]. Further, Mal et al. adopted transition metal catalyst dehydrogenation of AB blend of AB and *sec*-butyl amine borane in imidazolium based IL [22]. Rekken et al. took a different approach of IL facilitated dehydrogenation of amine boranes [23]. They synthesized task-specific ILs with the facile functionalization of N-substituted amine boranes.

Central cationic heteroatoms like phosphorous based ILs are relatively less explored in comparison with nitrogen based imidazolium, ammonium or pyrrolidinium based ILs [24]. So far, there is only one literature cited using Tetrabutylphosphonium chloride IL as solvent [18]. Phosphonium based ILs are another class of cations, which are relatively inexpensive compared to imidazolium based ILs [25,26]. The phosphonium based ILs have been used as super capacitors [27] and battery electrolytes [28] for their enhanced electrochemical window. Blundell and Licence conducted XPS analysis of a series of analogous phosphonium and ammonium ILs to determine cation-anion interactions [24]. In their work, the phosphonium based cations were found to have superior physiochemical properties such as thermal stability, viscosity, electrochemical stability, ionic conductivity over its ammonium counterparts. Industrial scale preparation of phosphonium ILs is reported by Bradaric et al. [29]. Tetrabutylphosphonium chloride IL has been used as novel phosphorous source and reaction medium to synthesize various phosphides which are later applied in hydrogen evolution reaction [30]. Apart from ILs, transition metal phosphide catalysts are being widely used as hydrogen evolution reaction [31,32].

Here we report the dehydrogenation of AB facilitated by the phosphonium based IL. The gas burette measurement gives the equivalent hydrogen generation. The intermediates and dehydrogenated products are characterized by ^{11}B nuclear magnetic resonance (NMR) spectroscopy. The role of IL is then confirmed by ^{1}H NMR characterization. High resolution mass spectrometry (HR-MS) characterization is further used to determine the mass of dehydrogenated oligomers. Finally, we propose the dehydrogenation mechanism based on dual NMR and HR-MS characterizations.

MATERIALS AND METHODS

1. Computational Method

The COSMO-SAC calculation for the prediction of IDAC of AB in IL requires COSMO files which are generated from two-step quantum chemical calculations. Initially, molecules, drawn by Gauss view 5.0 [33] visualization package, are geometry optimized in Gaussian 09 [34] package. Density functional theory (DFT) comprised of Becke's three-parameter exact exchange functional coupled with Lee, Young, Parr's gradient-corrected functions abbreviated as B3LYP [35,36] and 6-311+G(d) basis set are used for geometry optimization. Later, with the help of BVP86 [37] level of theory and another set of DFT calculations, COSMO files are generated from the optimized geometries. In the second calculation, density fitting basis set DGA1 [38] along with SVP [39] basis set are used for the accuracy in molecular structure and relative energy. The COSMO calculation divides molecules into certain number of tiny surface segments, whereby the surface area and screening charge densities are stored in COSMO files. Later, the COSMO files are used in our in-house reimplementation of COSMO-SAC program [40] to predict the IDAC.

However, a selection of cation and anion needs to be explored through quantum chemical models, as experiments are time consuming and often expensive. One such platform belongs to the use of **C**onductor like **S**creening **MO**del **S**egment **A**ctivity **C**oefficient (COSMO-SAC) model. This model can predict the infinite dilution activity coefficient (IDAC) values or the limit where the mole fraction of solute tends to be zero. These values are measurable and often are used as screening criteria. With the results discussed later, we have indeed been able to converge upon the selected IL, namely, Trihexyl(tetradecyl)phosphonium bis (2,4,4-trimethylpentyl) phosphinate ([TDTHP][Phosph]). This is an asymmetrical phosphonium IL that is useful for the solvation of AB and its subsequent dehydrogenation. This can be ascribed to the fact that [TDTHP][Phosph] is basic in nature and is known to stabilize the intermediates in other amine borane dehydrogenations [41,42].

2. Experimental Method

[TDTHP][Phosph] (≥95% purity) and AB (97% purity) were purchased from Sigma Aldrich. Impurities present in ILs were removed by keeping the ILs in an oil bath for 48 hours at 80 °C. The experimental setup for dehydrogenation experiment is given in Fig. 1(a). The setup is divided into gas side and reactor side. Reactor side contains two-necked reactor and two filter valves (S1 and S2) and a gas collection section. Here S2 is connected by vacuum pump through O3 valve. For the dehydrogenation experiment, high vacuum at the very initial stage removes the moisture and volatile matter (if any) remaining in IL. This ensures to minimize the effect of oxygen and moisture in the system which can influence reaction dynamics. The S1 and S2 valves remain closed during heating, and after a certain time period, evolved gases are allowed to pass through S1 and to enter into condenser. The red arrows indicate the flow path of gas. The condenser is a concentric tube where the inner tube contains liquid nitrogen and outer tube allows the gases from the reactor. Liquid nitrogen acts as cold trap as it condenses most of the volatiles and moisture (if present) during dehydrogenation, allowing only the hydrogen to pass to gas chamber (GC). The condensate is drained out from outlet (O1) after opening the S3 valve. During the dehydrogenation it remains closed. Being the lightest element, hydrogen gas passes through condenser and enters into the gas chamber (GC). Finally, the volume of hydrogen is measured by the displacement of mercury in gas burette. During the heating period, all valves remain closed. However, after the hydrogen gas enters into GC, O2 is opened up to allow atmospheric air, which creates barometric pressure on mercury in mercury bottle. This causes rise of mercury in the gas burette. The GC is also a concentric tube (not shown in diagram) whose inner one is connected with condenser outlet (S4) and outer one is connected with O2. Thus the atmospheric air enters through O2, does not mix with hydrogen. After the measurement, O2 is closed and S6 is opened to bring mercury down. Later, the vacuum cycle is performed to

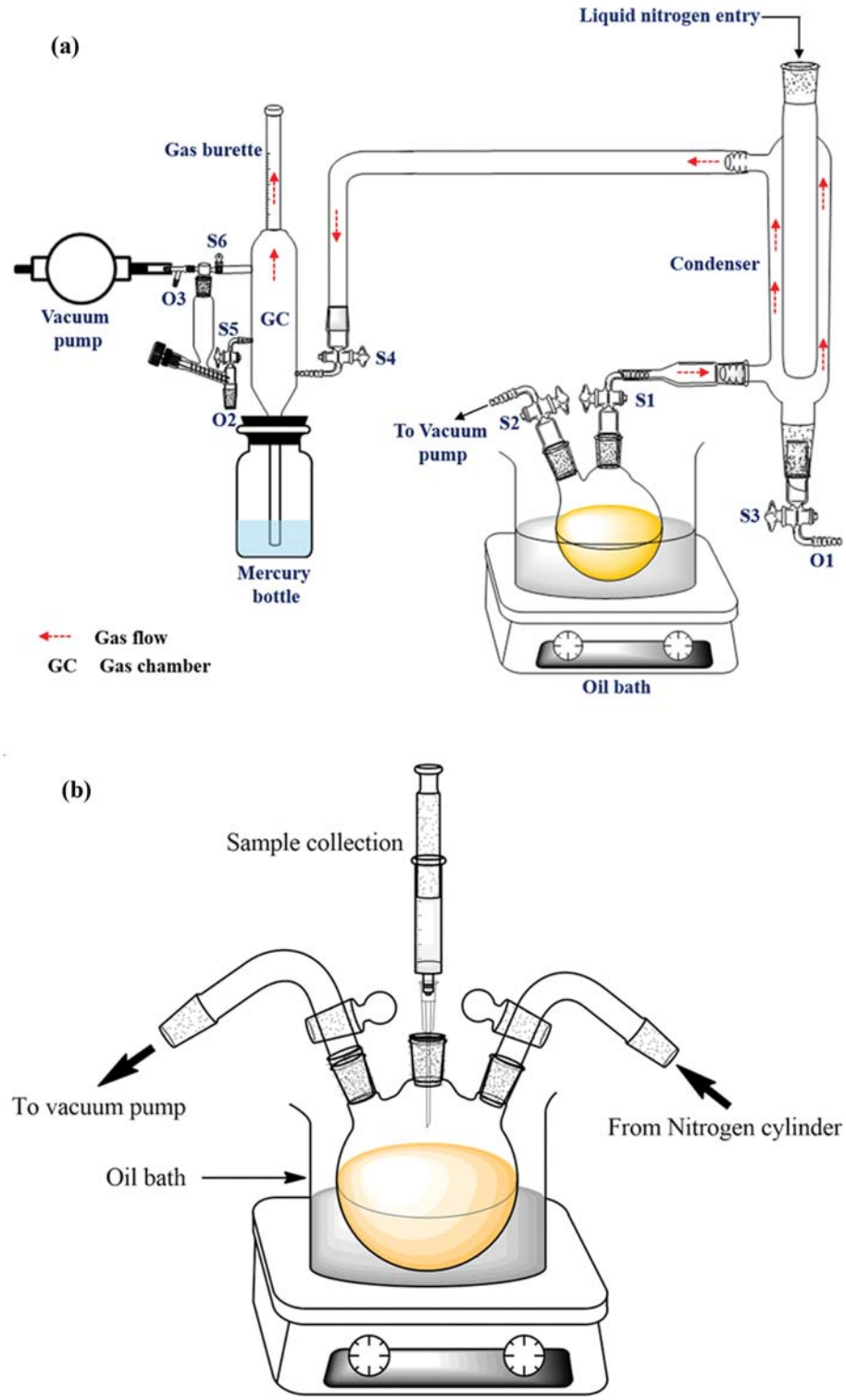

Fig. 1. Experimental setup: (a) Schematic diagram of experimental setup for dehydrogenation experiment, (b) experimental setup for collecting aliquots, Reprinted (adapted) [42] with permission from Copyright (2018) American Chemical Society.

remove the gases and the dehydrogenation process is repeated. The purity of hydrogen is checked by gas chromatography analysis (Bruker, 450-GC, column Carboxen), collecting H_2 gas from the top of gas burette by a Hamilton gas syringe (5 mL, 22/2′/2). During dehydrogenation, the entire setup is maintained at vacuum mentioned above to avoid erroneous measurement at gas burette.

For a typical dehydrogenation run, 10 mg of AB and 0.5 ml vacuum dried IL are taken in a three-necked reactor kept in oil bath at 105 °C and 4×10^{-2} mbar (±4% instrument error) gauge pressure. Such amount of AB is taken due to the limitation of our experimen-

Table 1. Infinite dilution activity coefficient of AB in phosphonium based ILs predicted by COSMO-SAC

Phosphonium Ionic liquid	ln (IDAC)
Tetrabutylphosphonium methansulfonate	−2.96
Tetrabutylphosphonium tetrafluroborate	−5.22
Tetrabutylphosphonium p-toluenesulfonate	−9.68
Tributylmethylphosphonium dibutyl phosphate	−14.75
Tributylmethylphosphonium methyl sulfate	−6.90
Triethylmethylphosphonium dibutyl phosphate	−14.99
Trihexyltetradecylphosphonium bis (trifluoromethyl-sulfonyl) imide	6.35
Trihexyl(tetradecyl)phosphonium bis (2,4,4-trimethylpentyl) phosphinate	−18.39
Trihexyltetradecylphosphonium bromide	−14.94
Trihexyltetradecylphosphonium chloride	−21.55
Trihexyltetradecylphosphonium dicyanamide	−5.95

tal setup. In this scenario, equivalent amount of hydrogen evolved per mole of AB fed to the system is more appropriate. The rise of mercury compresses hydrogen in the gas burette and volume of hydrogen is noted. The volume of hydrogen is converted to equivalent moles of hydrogen evolved. Therefore, the moles of hydrogen is divided with the moles of AB to calculate equivalent amount of hydrogen generated per mole of AB.

However, the setup is inadequate for collecting aliquot during runtime of the reaction because of high vacuum. Hence, to collect aliquots for NMR characterization, the three-necked reactor is kept in nitrogen atmosphere as shown in Fig. 1(b). 100 mg of AB and 5 ml of IL are kept at T=105 °C. The aliquots are collected at a specified interval of reaction with the help of syringe. After each sample collection, the evolved gas and nitrogen are pumped out to minimize the influence of evolved gases, thereafter the reactor is again filled up by nitrogen. NMR characterization is performed on a 600 MHz NMR spectrometer (Bruker, AVANCE III HD, software Topspin 3.5), where deuterated chloroform (99.8 atom % D, contains 1% (v/v) TMS, $CDCl_3$) is used as NMR solvent. High resolution mass spectra are recorded in +APCI mode on an Agilent Accurate-Mass Q-TOF LC/MS 6520 where the peaks are given in m/z (% of basis peak) with methanol (HPLC grade) as solvent. The molecular motion of AB is hindered by viscous nature of IL. Hence the viscosity of IL and AB/IL systems is measured with an interfacial rheometer (Anton Paar, Physica MCR301), having a gap between rheometer geometry plates of about 0.1 mm.

RESULTS AND DISCUSSION

1. Screening of ILs

The combination of cations and anions creates a large number of possible IL formations. However, as we are focusing on phosphonium based ILs due to their inherent advantages as compared to imidazolium ones, we have considered 11 phosphonium based ILs which are available commercially. Here the key to dehydrogenation is the breaking of the dihydrogen bond network. The polar cations and anions attack the hydridic and protic moieties of AB. The stronger the attraction, greater the solvation of AB in IL and higher the ease of dehydrogenation. To observe such a phenomenon, we have employed a quantum chemical based COSMO-SAC model to predict the infinite dilution activity coefficient (IDAC) of AB in 11 phosphonium based ILs as listed in Table 1. The logarithmic IDAC {ln(IDAC)} is a quantitative descriptor of solubility of solute in solvent. Higher the negative value of ln(IDAC), the more soluble is AB in IL. On the other hand, insolubility is defined by its positive value. Although AB has the highest logarithmic IDAC in trihexyltetradecylphosphonium chloride of −21.55, we do not consider the halogen base ILs because of the formation of acids upon heating by the IL itself. AB has logarithmic value of IDAC of −18.39 in [TDTHP][Phosph], and therefore was considered for our experiments.

2. NMR Characterization

Solid pure AB releases hydrogen via three distinct steps: induction, nucleation and growth [43]. The dihydrogen bonding network prevents the release of hydrogen instantly upon heating. The prolonged heating at 85 °C for 3 hours creates a mobile AB phase which disrupts the hydrogen bond network. The mobile AB phase also paves the way of bimolecular addition of AB. The bimolecular intermediate is known as diammoniate diborane {$[(NH_3)_2BH_2^+][BH_4^-]$, DADB} and is believed to release first equivalent of hydrogen. The formation of DADB from mobile AB phase is considered as a reversible reaction where protic and hydridic moieties are considered to be more reactive than that of AB. The lower energy barrier facilitates the addition of AB in DADB. The subsequent release of hydrogen is therefore termed as growth phase of dehydrogenation. This implies that the dehydrogenated non-volatile product at the growth phase is a complex mixture of polyaminoborane (PAB). After releasing the second hydrogen, PAB forms crosslinked polyiminoborane (PIB) or polyborazylene (PB). Theoretically, three molecules of hydrogen can be released from AB to form boron nitride (BN). However, BN is considered as a thermodynamic sink and cannot be converted back to AB [44]. Hence, the aim is to restrict the dehydrogenation up to the formation of PB.

The evolution of various boron moieties during dehydrogenation of AB in [TDTHP][Phosph] is characterized by ^{11}B NMR. Since IL contains no boron, a time resolved ^1H NMR characterization was performed to characterize IL during dehydrogenation. First, we performed temperature resolved characterization of AB/[TDTHP][Phosph] system after 1 min of heating at 60, 80, 90 and 105 °C (Fig. S1 of supporting information). Fig. 2 represents the time resolved

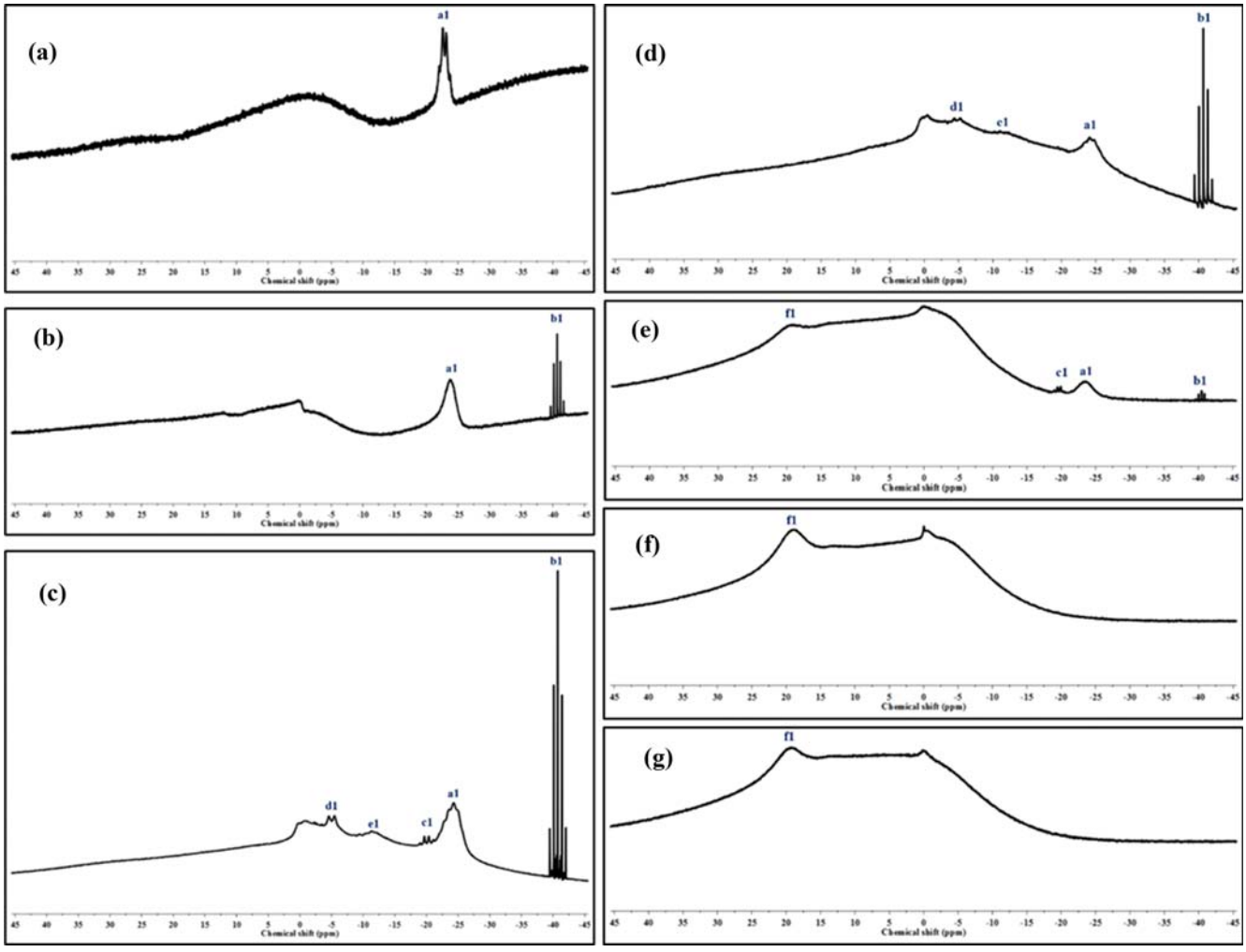

Fig. 2. ^{11}B NMR of AB/[TDTHP][Phosph]. (a) 0 min, (b) 1 min, (c) 10 min, (d) 20 min, (e) 30 min, (f) 60 min, (g) 240 min.

^{11}B NMR of AB/[TDTHP][Phosph] system at 105 °C. The chemical shift at δ=−23.82 ppm (denoted by '**a1**') represents -BH_3 moiety. After 1 min of heating at 105 °C, a new resonance at δ=−40.69 ppm (denoted by '**b1**') appeared along with -BH_3 resonance. The sharp quintet shaped (five parallel lines) was assigned to -BH_4^- moiety from DADB, and thus the absence of induction period was confirmed. After 10 min of dehydrogenation (Fig. 2(c)), we observed additional resonances at δ=−5.46, −11.28 and −20.36 ppm. The appearance of chemical shifts is greatly influenced by the reaction environment. For pure AB dehydrogenation, the appearance of -BH_2 was observed at δ=−13 ppm in the induction phase [43]. However, during nucleation phase, it was observed between δ=−10 to −14 ppm. The presence of polar moieties of IL facilitates shifting of -BH_2 resonance where it is assigned at δ=−5.46 ppm (denoted by '**d1**'). At δ=−20.36 ppm (denoted by '**c1**'), the quartet resonance is assigned to the new phase of -BH_3 moiety of AB. The new phase echoes the findings of Stowe et al. [43] Further, broad resonance at δ=−11.28 ppm (denoted by '**e1**') refers to the formation of polyaminoborane (PAB). It has been argued that the resonance of PAB extends from δ=−7 to −25.1 ppm [9] However, PAB, a linear oligomer, consists of linear dimer of -BH_2 moiety, which is observed at δ=−12.1 ppm [43]. Considering these discussions, the multiplet at δ=−11.28 ppm was assigned for PAB. The presence of these spectra was further observed after 20 min of dehydrogenation (Fig. 2(d)). Thus, the reaction equilibrium shifts towards the release of first equivalent of hydrogen and in the subsequent start of the propagation stage. However, unlike the dehydrogenation of AB in imidazolium based ILs where AB is totally converted to DADB, followed by formation of PAB, the basic environment of phosphonium based IL slows down the conversion of AB to DADB. After 30 min (Fig. 2(e)), resonance at δ=19.5 ppm appeared. The dehydrogenation of AB is known to form unsaturated sp^2 B=N framework after prolonged heating. Here the unsaturated framework refers to the formation of polyborazylene, since IL facilitates dehydrogenation suppressing other B=N species [9,14]. Further, they argue that solution phase ^{11}B NMR in presence of IL, the chemical shift of B=N is observed at δ=16 ppm. However, for pure component dehydrogenation, this was observed at δ=~30 ppm. Therefore, a 14 ppm upfield shift is possible for IL assisted dehydrogenation. Note that the probe temperature of NMR measurement significantly affected the location of resonances. The resonance at δ=16 ppm could be shifted to δ=~30 ppm region if the probe is heated to 100 °C [9].

Therefore, shifting of resonances is a very realistic fact to consider and we refer δ=19.57 ppm (denoted by '**f1**') as sp^2 unsaturated B=N moiety of polyborazylene. However, after 60 min, we only observed the resonance for B=N at δ=18.88 ppm, claiming the end of dehydrogenation reaction (Fig. 2(f)). Long-term heating up to 240 min does not produce new resonances (Fig. 2(g)). In the ^{11}B NMR spectra, resonance is observed at δ=0 ppm, which refers to the spectra of borosilicate NMR tube we were using for characterization.

We further inspected the ^{1}H NMR spectrum to reveal the role of IL in dehydrogenation. The chemical shift corresponding to each hydrogen of IL is calculated by determining the area under the curve of each peak and relating it with the number of hydrogens attached to a particular moiety [41]. At first, a unity area, corresponding to a hydrogen, is identified and referred as resonance. Corresponding to the reference, other areas are integrated and hydrogens of other moieties are located. The shielding effect of nuclei is also taken into consideration while assigning a moiety. Fig. 3

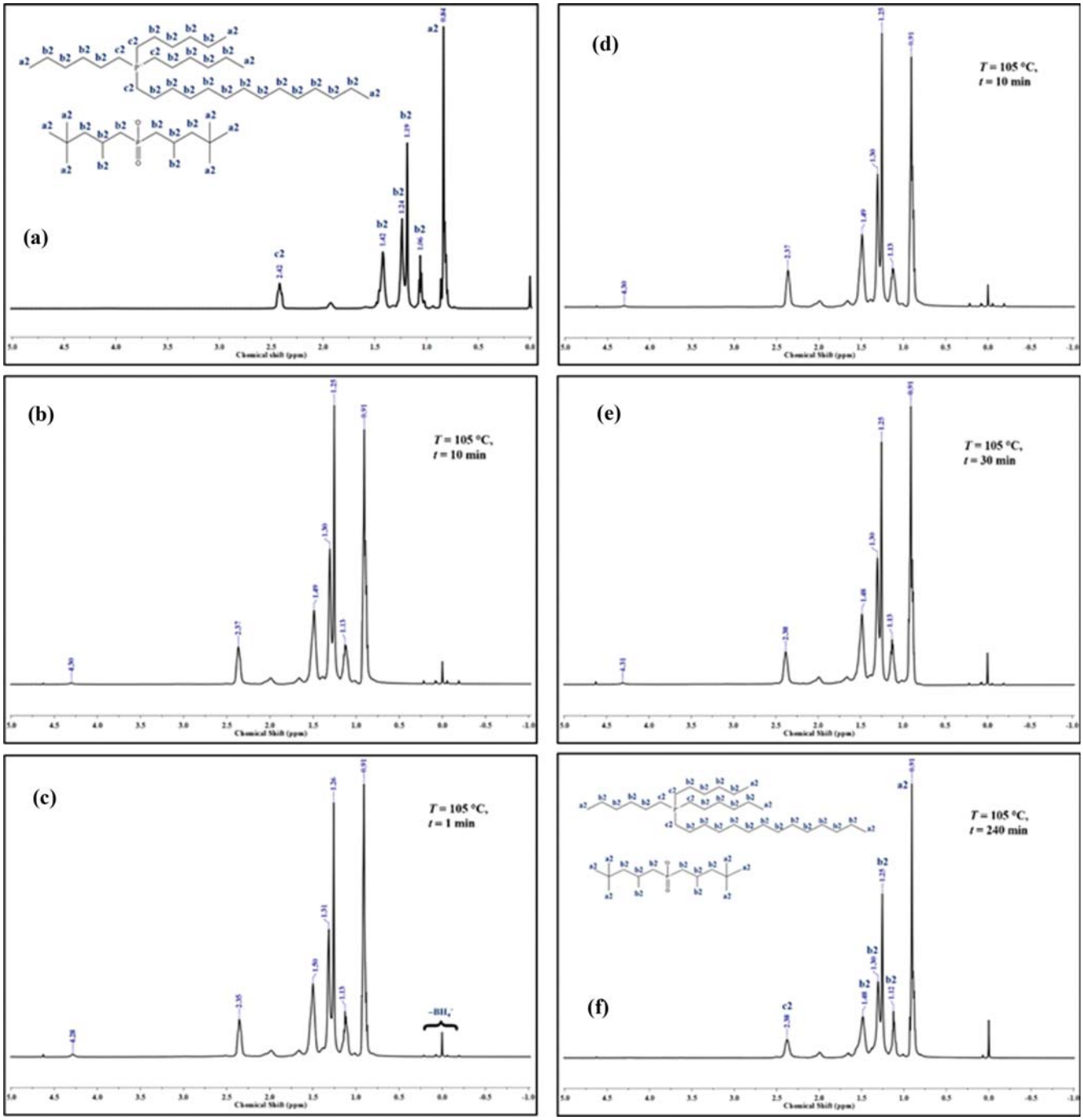

Fig. 3. ^{1}H NMR of pure [TDTHP][Phosph] (a) and AB/[TDTHP][Phosph] ((b)-(f)). (a) Pure [TDTHP][Phosph], (b) 0 min, (c) 1 min, (d) 10 min, (e) 30 min, (f) 240 min.

represents the ^{1}H spectra of pure [TDTHP][Phosph] and the time resolved ^{1}H NMR spectra of AB/[TDTHP][Phosph] system at 0 min (before reaction), 1, 10, 30, 240 min. In Fig. 3(a), the terminal -CH_3 moieties of cation and anion are sp^3 and most shielded. Therefore, the chemical shift at δ=0.86 ppm corresponds the -CH_3 moiety of IL (denoted by '**a2**'). The chemical shift of δ=1.06-1.42 ppm is assigned to -CH_2 moieties of IL (denoted by '**b2**'). Similarly, the deshielded hydrogens at α-carbon of cationic center will have downfield deflection, and hence δ=2.42 ppm is assigned (denoted by '**c2**'). Upon solvation of AB in IL, upfield shift of '**c2**' is observed whereas other methyl moieties are shifted to downfield position. Due to the presence of electronegative nitrogen atom, chemical shift of -NH_3 moiety of AB was observed at δ=4.35 ppm. The chemical shift of -NH_3 was seen to decrease over 1, 10 and 30 min spectrum. During dehydrogenation, Fig. 3(b)-(e), a quintet resonance at δ=−0.19 to 0.22 ppm refers to -BH_4^- anion. The observance of -BH_4^- at 1 min echoes the findings of ^{11}B NMR spectra. However after 240 min, the resonances of AB disappear and chemical shift of system (Fig. 3(f)) resembles that of pure IL. This confirms the structural integrity of IL during dehydrogenation. Therefore, in addition to solvation, the [TDTHP][Phosph] IL further acts as a liquid catalyst.

3. HR-MS Characterization

Fig. 4 represents the HR-MS analysis of dehydrogenated AB/[TDTHP][Phosph] system in positive APCI mode. The analysis of mass spectra reveals the exact mass of compounds formed. Four distinctive peaks are identified in Fig. 4. The peak corresponding to phosphinate anion is assigned as 291.24. This corresponds to the calculated mass for phosphinate anion ($[M+H]^+$), which is 289.23. The corresponding peak for $[TDTHP]^+$ is assigned at 483.53, as the calculated mass for cation ($[M+H]^+$) is 483.50. The HR-MS characterization also supports the structural integrity of IL as characterized by NMR. The two other peaks '**c3**' and '**d3**' are referred to polymeric structure of polyborazylene. From the ^{11}B NMR, we confirm the B=N containing oligomers from [TDTHP][Phosph] facilitated dehydrogenation. The nearest chemical formula of PB oligomer corresponding to peak 581.48 is $B_{22}H_{19}N_{23}$ having a calculated mass of 583.42. Similarly, corresponding to 871.72 peak, the chemical formula corresponds to a calculated mass of 872.59 with a chemical formula of $B_{34}H_{22}N_{34}$. Hence, the dehydrogenation leads to a mixture of polymeric product. The growth of the chain depends on the stabilization of intermediates in IL environment. In summary, the phosphinate based ILs are basic in nature and -BH_4^- anion are found to be more stable in nucleophilic condition.

4. Equivalent Hydrogen Production

The dehydrogenation experiment was carried out at 105 °C and 4×10^{-2} mbar (±4% instrument error) gauge pressure. A set of three experiments were performed to ensure repeatability. An average cumulative equivalent hydrogen with progress of time is given in Fig. 5. After 240 min of dehydrogenation, 2.07 equivalent of hydrogen was produced from AB/[TDTHP][Phosph] system. We observed a high amount of hydrogen release up to 40 min of experiment where nearly 2.0 equivalent of hydrogen was released. After 60 min, the curve becomes almost parallel to the time-axis, resulting in negligible release. The release kinetics supports our ^{11}B NMR observation where virtually no change in resonance spectrum was

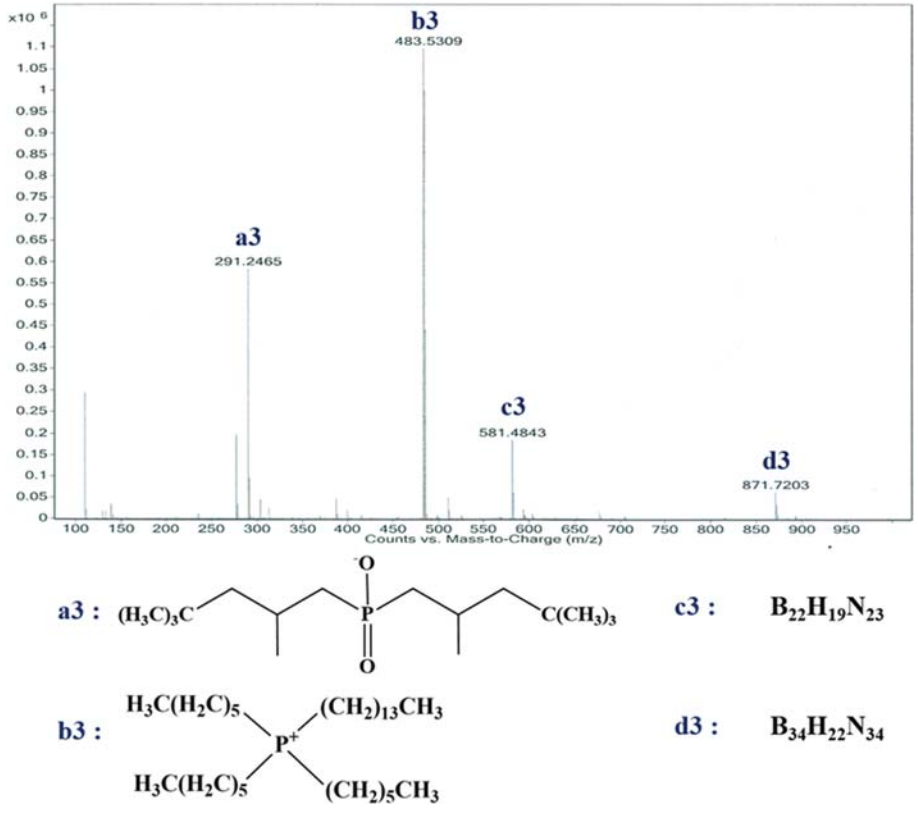

Fig. 4. APCI-HR-MS plot of AB/[TDTHP][Phosph] after reaction.

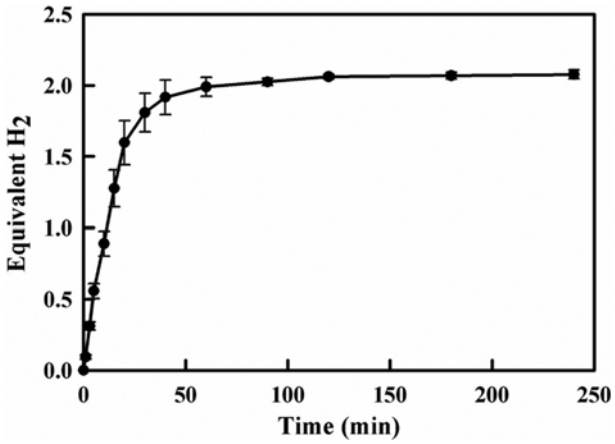

Fig. 5. Time resolved equivalent hydrogen release from AB/[TDTHP][Phosph] at 105 °C.

observed after 60 min and the second hydrogen release practically indicates the formation of B=N moiety. Initially, 0.89 equivalent of hydrogen was released after 10 min of dehydrogenation, i.e., the conversion of DADB to PAB was initiated after the release of the first hydrogen. However, the conversion accelerated between 10-30 min where DADB gets entirely converted. Thereafter, PAB loses its second hydrogen to form PIB or PB. However, at this stage, our gas burette measurement showed relative inconsistency in data and an approximately 0.15 standard deviation was observed.

5. Proposed Dehydrogenation Mechanism

Based on the dual characterization of ^{11}B NMR and HR-MS analysis, we propose a reaction mechanism of [TDTHP][Phosph] facilitated dehydrogenation of AB. As ^{1}H NMR proves no structural changes of IL, i.e., acting as a catalytic agent and solvent, the proposed mechanism is detailed without the structure of IL. The use of [TDTHP][Phosph] IL effectively suppresses the induction period by dissolving the AB at higher temperature. Hence, it can be assumed that the bimolecular mobile AB phase is readily formed due to the polar nature of AB as -BH_4^- is detected after 1 min (step 6.1 and 6.2 of Fig. 6). The appearance of -BH_4^- anion after 1 min of dehydrogenation suggests the absence of induction period of [TDTHP][Phosph] facilitated dehydrogenation. However, the resonance is not present after 1 min at 60, 80, 90 °C. We refer to the viscosity of the system that hampers the effective reorientation of cations and anions with hydridic and protic moieties. Fig. 7 represents the temperature varied viscosity of IL and AB/IL systems. The viscosity of pure [TDTHP][Phosph] is 365.5 mPa s at 25 °C, which reduces to 14.93 mPa s at 105 °C. However, upon addition of AB, the viscosity reaches 854.63 mPa s at 25 °C and 34.99 mPa s at 105 °C. Further, we observed drastic reduction of AB/IL system at 40 °C. The ionic moieties of IL attract the protic and hydridic moieties through nonbonded interactions which require close proximity of IL. With the increase in temperature, the viscosity reduces, ionic mobility increases and thus probability of nonbonded interaction increases. The increased interaction facilitates to break the dihydrogen bonding of AB and induction period is suppressed. In the nucleation phase, the formation of DADB reduces the activation energy barrier and propagates the reaction in forward direction. The presence

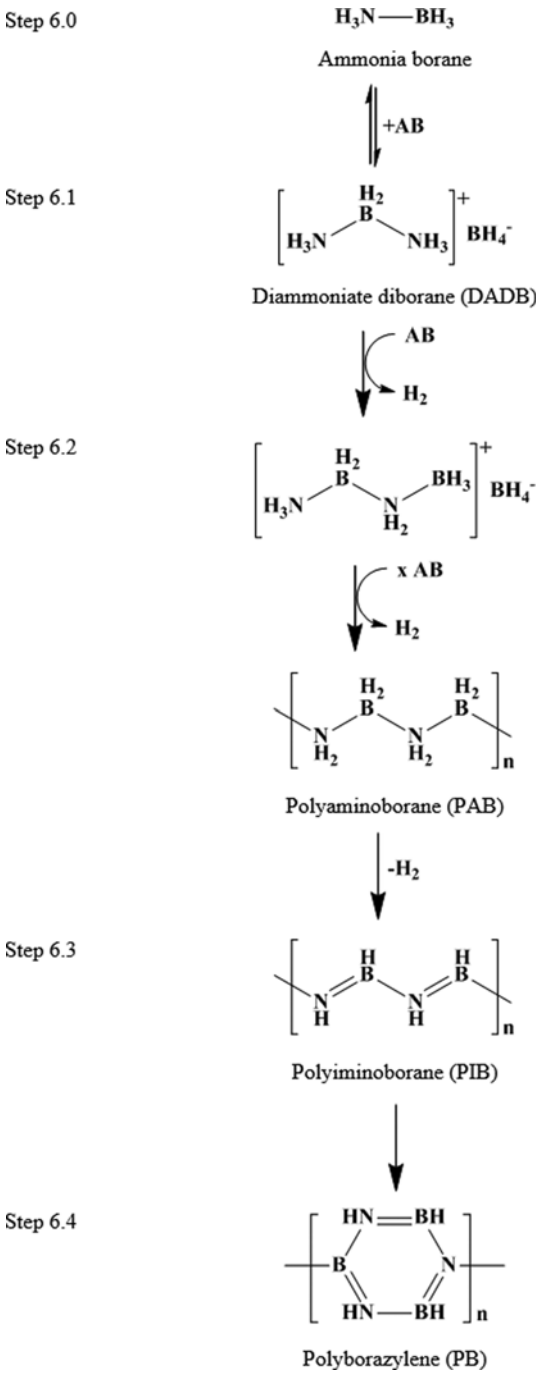

Fig. 6. Proposed dehydrogenation pathway of AB/Phosphonium IL.

of resonance for -BH_3 moiety at 30 min (refer to '**a1**') suggests that all AB molecules do not get dimerize to form DADB. DADB is an important precursor to form polyaminoborane in the growth phase. Once the DADB forms, the activation energy barrier is reduced and first equivalent hydrogen is released. In the growth phase, AB monomers are attached to the DADB to form oligomeric chains. However, the addition of AB happens through the generation of -BH_4^- anion (step 6.2). For that, we observe the resonance for -BH_4^- at δ=–39.46 ppm up to 30 min. The simultaneous presence of resonances for DADB and PAB ('**b1**', '**d1**' and '**e1**') concludes the active

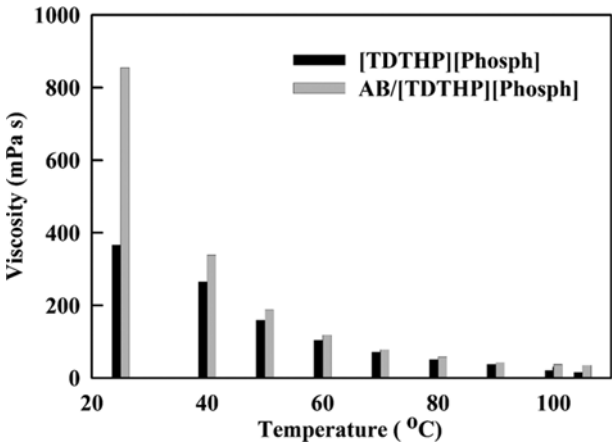

Fig. 7. Viscosities of IL and AB/IL systems. For measurement of IL, 0.5 mL IL is taken and for measurement of AB/IL system, 10 mg AB is mixed with 0.5 mL of IL.

nature of DADB intermediate. This initiates the forward direction. Similarly, once PAB is formed, it converts to PIB by losing second equivalent of hydrogen (step 6.3), which again rearranges itself to generate PB (step 6.4). The presence of PIB as intermediate of PB formation from PAB is also discussed by Himmelberger et al. [9]. Overall, from our dehydrogenation experiment, ~2.0 equivalent of hydrogen was evolved within 50 min of experiment, i.e., referring to a fast dehydrogenation mechanism with [TDTHP][Phosph] IL. Unlike the dehydrogenation of pure AB, the IL solvation suppresses the side product formation, which includes both volatile and non-volatile components. Further, it is seen to selectively produce polyborazylene, which tends to control the extent of reaction. The entire mechanism is described in Fig. 6.

6. Comparison with Literature

As seen in Table 2, significant effort and progress has been made into making IL as viable scaffold of AB for hydrogen production. However, most of the effort is put into imidazolium class of IL as

Table 2. Comparison of ionic liquid facilitated dehydrogenation of ammonia borane with literature

Article	Name of the ILs*	Dehydrogenation condition	Yield of hydrogen and other major outcome	Reference
Bluhm et al., 2006	[BMIM][Cl]	1 : 1 weight ratio of AB and IL in a vacuum reactor at 85, 90, 95 °C	• 0.5, 0.8 and 1.1 equivalent of H_2, after 1 hour at 85, 90, and 95 °C, respectively • 0.95, 1.2 and 1.5 equivalent H_2 after 3 hour for the same temperature range • 1.2, 1.4, and 1.6 equivalent of H_2 after 22 hour of reaction	14
Himmelberger et al., 2009	[BMIM][Cl], [BMIM][I], [BMMIM][Cl], [BMIM][BF_4], [BMIM][OTf], [BMIM][PF_6], [EMMIM][$EtSO_4$], [EMMIM][OTf], [MMIM][$MeSO_4$], [PMMIM][Tf_3C]	Dehydrogenation reaction is in nitrogen atmosphere within a temperature range of 75-120 °C	• AB/[BMIM][Cl] system releases 1.0 equivalent of H_2 in 67 min and 2.2 H_2 equivalent in 330 min • Presence of DADB is confirmed by ^{11}B NMR • Subsequent dehydrogenation leads to form poly(aminoborane) and polyborazylene	9
Al-Kukhun et al., 2011	[BMIM][Cl]	Reaction for 20 min at 110 °C at argon environment of 1 atmosphere pressure	• In absence of moisture, AB/[BMIM][Cl] releases 5.7 wt% H_2, with 0.08% AB conversion to ammonia and 0.07 mol% NH_3 in gas phase	3
Ahluwalia et al., 2011	[BMIM][Cl]	85-95 °C in high vacuum	• Dehydrogenation kinetics is modeled by modified Avrami-Erofeyev model • Complete conversion of AB is achieved with more than 200 °C • Design of non-isothermal plug flow reactor and flow reactor for possible scale up	16
Wright et al., 2011	[BMIM][Cl], [BMMIM][Cl], [EMMIM][$EtSO_4$], [BMIM][Tf_2N]	Ruthenium catalyst supported dehydrogenation below 85 °C	• AB/[BMIM][Cl] has initial higher H_2 release rate at 45 and 65 °C but overall yield of lower amount of H_2 released • Similar steady increment is reported for AB/[EMMIM][$EtSO_4$]	21
Mal et al., 2011	[EMIM][$EtSO_4$]	Ruthenium catalyst supported dehydrogenation at 80 °C in dry nitrogen environment	• 3.4 wt% H_2 at 80 °C within 4 hour and 3.6 wt% H_2 in 18 hour, without formation of insoluble poly(aminoborane)	22

Table 2. Continued

Article	Name of the ILs*	Dehydrogenation condition	Yield of hydrogen and other major outcome	Reference
Rekken et al., 2014	N-substituted amine-borane ionic liquids (N-ABILs)	Dehydrogenation for 8 hour, at 130 °C and a pressure of 9 bar in nitrogen atmosphere	• From pure N-ABILs, 2.0 equivalent of H_2 produced with <1% impurity • N-ABILs blended with AB produces 2.3 equivalent of H_2 per mole of AB	23
Valero-Pedraza et al., 2015	[BMIM][Cl], [AMIM][Cl], [HOEMIM][Cl], [EMIM][Cl], [EMIM][OAc], [P_{4444}][Cl], [Ch][H_2PO_4], [Ch][OAc], [Ch][Tf_2N], [EMIM][OTf], [EMIM][Tf_2N], [EMIM][$EtSO_4$], [EMPy][Tf_2N]	10 wt% AB in ILs at 85 °C (±1 °C certainity) and 10 mbar absolute pressure	• [EMIM][Tf_2N] facilitated system releases 0.5 equivalent of H_2 at 85 °C within 5-15 min of reaction • Soluble residue is formed after dehydrogenation	18
Gatto et al., 2017	[BMPyr][Tf_2N], [DEBA][Tf_2N], [DMPA][Tf_2N]	Case 1: 70 mass% AB and 30 mass% IL, Case 2: 77 mass% AB and 23 mass% IL	• Lowers dehydrogenation temperature of less than 90 °C • Improved dehydrogenation kinetics without induction period	19
Present study	[TDTHP][Phosph]	Dehydrogenation at 105 °C and 4×10^{-2} mbar of gauge pressure	• 2.0 equivalent release within 40 min and 2.07 equivalent of hydrogen production after 240 min • Stable Polyborazylene formation after 30 min of reaction	---

[BMIM][Cl], 1-butyl-3-methylimidazolium chloride; [BMIM][I], 1-butyl-3-methylimidazolium iodide; [BMMIM][Cl], 1-butyl-2,3-dimethylimidazolium chloride; [BMIM][BF_4], 1-butyl-3-methylimidazolium tetrafluoroborate; [BMIM][OTf], 1-butyl-3-methylimidazolium triflate; [BMIM][PF_6], 1-butyl-3-methylimidazolium hexafluorophosphate; [EMMIM][$EtSO_4$], 1-ethyl-2,3-dimethylimidazolium ethylsulfate; [EMMIM][OTf], 1-ethyl-2,3-dimethylimidazolium triflate; [MMIM][$MeSO_4$], 1,3-dimethylimidazolium methylsulfate; [PMMIM][Tf_3C], 1-propyl-2,3-dimethylimidazolium triflide; [BMIM][Tf_2N], 1-butyl-3-methylimidazolium bis(trifluoromethylsulfonyl)imide; [AMIM][Cl], 1-allyl-3-methylimidazolim chloride; [HOEMIM][Cl], 1-(2-hydroxyethyl)-3-methylimidazolium chloride; [EMIM][Cl], 1-ethyl-3-methylimidazolium chloride; [EMIM][OAc], 1-ethyl-3-methylimidazolium acetate; [P_{4444}][Cl], tetrabutylphosphonium chloride; [Ch][H_2PO_4], choline dihydrogen phosphate; [Ch][OAc], choline acetate; [Ch][Tf_2N], choline bis(trifluoromethylsulfonyl)imide; [EMIM][OTf], 1-ethyl-3-methylimidazolium triflate; [EMIM][Tf_2N], 1-ethyl-3-methylimidazolium bis(trifluoromethylsulfanyl)imide; [EMIM][$EtSO_4$], 1-ethyl-3-methylimidazolium ethyl sulfate; [EMPy] [Tf_2N], 1-ethyl-3-methylpyridium bis(trifluoromethylsulfanyl)imide; [BMPyr][Tf_2N], 1-butyl-1-methylpyrrolidinium bis(trifluoromethylsulfonyl)imide; [DEBA][Tf_2N], *N*,*N*-dimethyl-*N*-ethyl-*N*-benzylammonium bis(trifluoromethylsulfonyl)imide; [DMPA][Tf_2N], *N*,*N*-diethyl-*N*-methyl-*N*-propylammonium bis(fluorosulfonyl)imide; [TDTHP][Phosph], trihexyl(tetradecyl)phosphonium bis (2,4,4-trimethylpentyl) phosphinate

it is seen to exert strong effect on the reaction kinetics and yield of H_2 when combined with basic anions [45]. The imidazolium IL facilitated dehydrogenation mostly follows the reaction mechanism depicted for the dehydrogenation of pure AB. However, other than imidazolium class of IL, no report provides detailed mechanistic insight on other classes of ILs, although very recently pyridinium, phosphonium, pyrolidinium, choline and ammonium based ILs are reported [18,19]. Based on the mechanistic investigation of AB/[BMIM][Cl] system, Ahluwalia et al. modelled the kinetics with modified Avrami-Erofeyev model [16]. The kinetic simulations elucidate the design of the reactor for a possible scale up. The detailed kinetic modelling further integrates the AB/IL system in proton-exchange-membrane fuel cells [3]. Keeping the technological advance in the background, we did a mechanistic investigation of AB/IL system with phosphonium based IL. The predictive screening approach saved time as well as expensive solubility experiments with various ILs. The detailed mechanistic investigation opens up pathways for the kinetic modelling of reactions and design of reactor. The combined experimental and modelling study would integrate this AB/phosphonium IL as a viable candidate for fuel cell system and on-board hydrogen storage system.

CONCLUSIONS

We present a detailed study of thermal dehydrogenation of AB facilitated by IL. The ^{11}B NMR characterization shows the absence of DADB formation upon heating at 60, 80, 90 °C, and after 1 min heating. Despite having a logarithmic IDAC of −18.39 as predicted by COSMO-SAC, the molecular motion of AB is hindered because of its high viscosity. Therefore, at 105 °C, with a reduced viscosity

of 34.99 mPa s, the protic and hydridic moieties make noncovalent interactions with IL species, ensuring a breakage of dihydrogen bonding. With the formation of DADB, AB molecule is added with DADB, leading to the formation of PAB after 10 min of reaction. The simultaneous presence of resonances at δ=−23.82 ppm, −40.69 ppm and −11.28 ppm confirms the presence of AB, DADB and PAB, respectively. These indicate that the entire AB is not readily converted to DADB in a single step. This leads us to propose the molecular AB addition in growth phase to form PAB. The B=N unsaturated moiety is seen to appear with PAB, confirming relative instability of PAB and second desorption of hydrogen. Thus, the [TDTHP][Phosph] provides a controlled reaction mechanism with a stable PB after 30 min. Even after prolonged heating to 240 min, broad resonance of PB does not get shifted into B-N moiety of boron nitride. HR-MS characterization further confirms the mass of oligomeric AB with selective number of repeat units instead of mixture of AB oligomers. The approximate formulas of PB as calculated from HR-MS analysis are $B_{22}H_{19}N_{23}$ and $B_{34}H_{22}N_{34}$.

ACKNOWLEDGEMENTS

The work reported in this article is financially supported by a research grant (SB/S3/CE/063/2013) under the Science and Engineering Research Board (SERB), Department of Science and Technology (DST), Government of India. The authors further acknowledge Central Instrument Facility of Indian Institute of Technology Guwahati and Central Instrument Facility of Indian Institute of Science Education and Research Bhopal for providing ^{1}H and ^{11}B NMR facilities, respectively. Due acknowledgments are also to the Analytical Laboratory of Department of Chemistry of IIT Guwahati for letting us record the HR-MS spectra.

SUPPORTING INFORMATION

Additional information as noted in the text. This information is available via the Internet at http://www.springer.com/chemistry/journal/11814.

REFERENCES

1. T. Richardson, S. de Gala, R. H. Crabtree and P. E. M. Siegbahn, *J. Am. Chem. Soc.*, **117**, 12875 (1995).
2. J. Li, F. Zhao and F. Jing, *J. Chem. Phys.*, **116**, 25 (2002).
3. A. Al-Kukhun, H. T. Hwang and A. Varma, *Ind. Eng. Chem. Res.*, **50**, 8824 (2011).
4. G. Cinti, D. Frattini, E. Jannelli, U. Desideri and G. Bidini, *Appl. Energy*, **192**, 466 (2017).
5. F. H. Stephens, V. Pons and R. T. Baker, *Dalton Trans.*, 2613 (2007).
6. A. Rossin and M. Peruzzini, *Chem. Rev.*, **116**, 8848 (2016).
7. A. Gutowska, L. Li, Y. Shin, C. M. Wang, X. S. Li, J. C. Linehan, R. S. Smith, B. D. Kay, B. Schmid, W. Shaw, M. Gutowski and T. Autrey, *Angew. Chem., Int. Ed.*, **44**, 3578 (2005).
8. H.-L. Jiang and Q. Xu, *Catal. Today*, **170**, 56 (2011).
9. D. W. Himmelberger, L. R. Alden, M. E. Bluhm and L. G. Sneddon, *Inorg. Chem.*, **48**, 9883 (2009).
10. M. A. P. Martins, C. P. Frizzo, D. N. Moreira, N. Zanatta and H. G. Bonacorso, *Chem. Rev.*, **108**, 2015 (2008).
11. T. Welton, *Chem. Rev.*, **99**, 2071 (1999).
12. R. M. Vrikkis, K. J. Fraser, K. Fujita, D. R. MacFarlane and G. D. Elliott, *J. Biomech. Eng.*, **131**, 074514 (2009).
13. C. V. Manohar, D. Rabari, A. A. P. Kumar, T. Banerjee and K. Mohanty, *Fluid Phase Equilib.*, **360**, 392 (2013).
14. M. E. Bluhm, M. G. Bradley, R. Butterick, U. Kusari and L. G. Sneddon, *J. Am. Chem. Soc.*, **128**, 7748 (2006).
15. T. Nakagawa, A. K. Burrell, R. E. Del Sesto, M. T. Janicke, A. L. Nekimken, G. M. Purdy, B. Paik, R.-Q. Zhong, T. A. Semelsberger and B. L. Davis, *RSC Adv.*, **4**, 21681 (2014).
16. R. K. Ahluwalia, J. K. Peng, and T. Q. Hua, *Int. J. Hydrogen Energy*, **36**, 15689 (2011).
17. S. Mahato, B. Banerjee, G. Pugazhenthi and T. Banerjee, *Int. J. Hydrogen Energy*, **40**, 10390 (2015).
18. M. J. Valero-Pedraza, A. Martín-Cortés, A. Navarrete, M. D. Bermejo and Á. Martín, *Energy*, **91**, 742 (2015).
19. S. Gatto, O. Palumbo, F. Trequattrini and A. Paolone, *J. Therm. Anal. Calorim.*, **129**, 663 (2017).
20. N. Sahiner and D. Alpaslan, *J. Appl. Polym. Sci.*, **131**, 40183 (2014).
21. W. R. H. Wright, E. R. Berkeley, L. R. Alden, R. T. Baker and L. G. Sneddon, *Chem. Commun.*, **47**, 3177 (2011).
22. S. S. Mal, F. H. Stephens and R. T. Baker, *Chem. Commun.*, **47**, 2922 (2011).
23. B. D. Rekken, A. E. Carre-Burritt, B. L. Scott and B. L. Davis, *J. Mater. Chem. A*, **2**, 16507 (2014).
24. R. K. Blundell and P. Licence, *Phys. Chem. Chem. Phys.*, **16**, 15278 (2014).
25. F. Atefi, M. T. Garcia, R. D. Singer and P. J. Scammells, *Green Chem.*, **11**, 1595 (2009).
26. R. E. Del Sesto, C. Corley, A. Robertson and J. S. Wilkes, *J. Organomet. Chem.*, **690**, 2536 (2005).
27. E. Frackowiak, G. Lota and J. Pernak, *J., Appl. Phys. Lett.*, **86**, 164104 (2005).
28. K. Tsunashima, and M. Sugiya, *Electrochem. Commun.*, **9**, 2353 (2007).
29. C. J. Bradaric, A. Downard, C. Kennedy, A. J. Robertson and Y. Zhou, *Green Chem.*, **5**, 143 (2003).
30. C. Zhang, B. Xin, Z. Xi, B. Zhang, Z. Li, H. Zhang, Z. Li and J. Hao, *ACS Sustainable Chem. Eng.*, **6**, 1468 (2018).
31. Y. Shia and B. Zhang, *Chem. Soc. Rev.*, **45**, 1529 (2016).
32. J. F. Callejas, C. G. Read, C. W. Roske, N. S. Lewis and R. E. Schaak, *Chem. Mater.*, **28**, 6017 (2016).
33. R. Dennington, T. Keith and J. Millam, GaussView (Version 5), Semichem Inc., Shawnee Mission, KS (2009).
34. M. J. Frisch, et al., Gaussian 09 (Revision D.01), Gaussian, Inc., Wallingford, CT (2013).
35. A. D. Becke, *J. Chem. Phys.*, **98**, 5648 (1993).
36. C. Lee, W. Yang and R. G. Parr, *Phys. Rev. B: Condens. Matter Mater. Phys.*, **37**, 785 (1988).
37. J. P. Perdew, *Phys. Rev. B: Condens. Matter Mater. Phys.*, **33**, 8822 (1986).
38. C. Sosa, J. Andzelm, B. C. Elkin, E. Wimmer, K. D. Dobbs and D. A. Dixon, *J. Phys. Chem.*, **96**, 6630 (1992).
39. A. Schäfer, H. Horn and R. Ahlrichs, *Chem. Phys.*, **97**, 2571 (1992).
40. A. Bharti, D. Kundu, D Rabari and T. Banerjee, Phase equilibria in

ionic liquid facilitated liquid-liquid extractions, CRC Press, New York (2017).
41. D. Kundu, B. Banerjee, G. Pugazhenthi and T. Banerjee, *Int. J. Hydrogen Energy*, **42**, 2756 (2017).
42. D. Kundu, S. Chakma, G. Pugazhenthi and T. Banerjee, *ACS Omega*, **3**, 2273 (2018).
43. A. C. Stowe, W. J. Shaw, J. C. Linehan, B. Schmid and T. Autrey, *Phys. Chem. Chem. Phys.*, **9**, 1831 (2007).
44. N. C. Smythe and J. C. Gordon, *Eur. J. Inorg. Chem.*, **2010**, 509 (2010).
45. S. Sahler, S. Sturm, M. T. Kessler and M. H. G. Prechtl, *Chem. Eur. J.*, **20**, 8934 (2014).

Supporting Information

Reactive insights into the hydrogen production from ammonia borane facilitated by phosphonium based ionic liquid

Debashis Kundu*, Sankar Chakma, Gopal Pugazhenthi*, and Tamal Banerjee*,†**

*Department of Chemical Engineering, Indian Institute of Technology Guwahati, Guwahati -781039, Assam, India
**Department of Chemical Engineering, Indian Institute of Science Education and Research Bhopal, Bhopal - 462 066, Madhya Pradesh, India
(*Received 27 August 2018 • accepted 25 November 2018*)

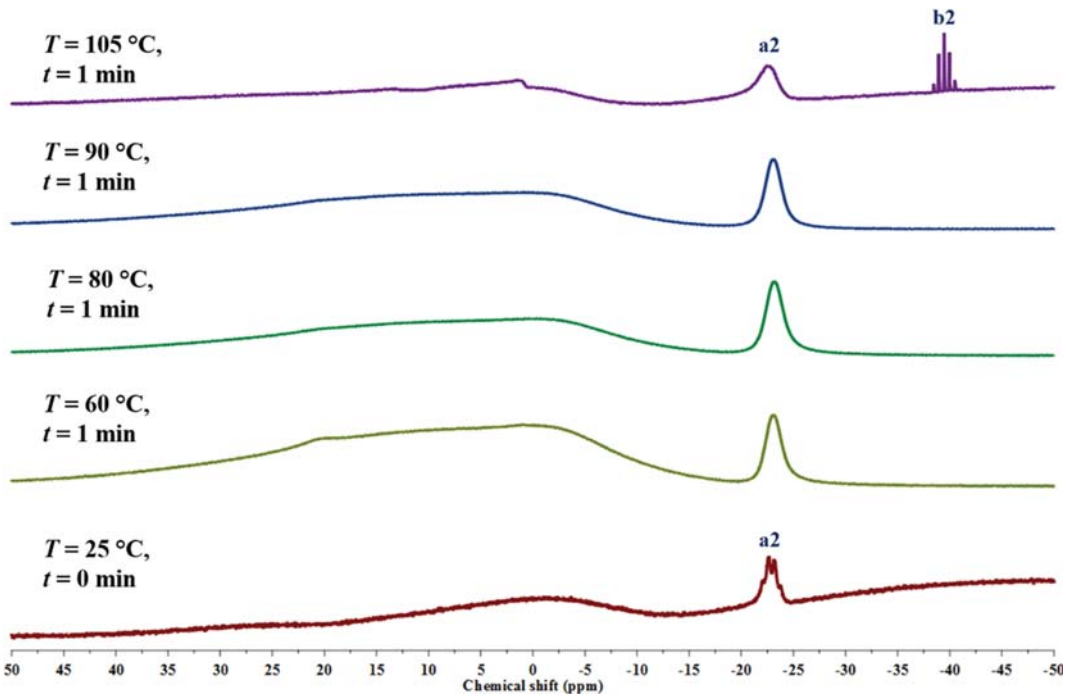

Fig. S1. ^{11}B NMR of AB/[TDTHP][Phosph] after 1 min. 'a2' denotes the -BH_3 moiety of AB and 'b2' denotes the -BH_4^- moiety of DADB.